Volume 68 • Issue 1 • January 2015

Journal of Achievements in Materials and Manufacturing Engineering

International Scientific Journal published monthly by the World Academy of Materials and Manufacturing Engineering

Etching techniques for duplex steels

P. Martínek*, P. Podaný

COMTES FHT a.s., Průmyslová 995, 334 41 Dobřany, Czech Republic

* Corresponding e-mail address: petr.martinek@comtesfht.cz

ABSTRACT

Purpose: This contribution describes a search for an optimum etching technique for duplex ferritic-austenitic steels which would enable metallographers to find the fractions of major phases by image analysis and determine the amounts, distributions and types of intermetallic phases.

Design/methodology/approach: The microstructures were revealed by etching with seven different reagents. The phase compositions were evaluated using either image analysis or test grid-based quantitative analysis. The experimental materials were X2CrNiMoN 22-5-3 steel and its cerium-doped variant. Each of them was examined in two conditions: upon open-die forging and subsequent solution annealing and upon long-time annealing, where the latter led to extensive precipitation of intermetallic phases. The fractions of major and intermetallic phases were also determined using EBSD. Both quantitative and qualitative EBSD data were then compared to the values obtained using optical microscopy.

Findings: In X2CrNiMoN 22-5-3 duplex steel, the microstructure can be revealed using various reagents and both chemical and electrochemical etching. The differences between the reagents, when used for evaluating the amounts of major phases (austenite + ferrite), were not substantial. The fraction of sigma phase in long-time-annealed samples can be evaluated using image analysis only if etched with NaOH solution or NH_4OH. These etchants also effectively reveal carbides on grain boundaries. However, the values obtained with NaOH are overestimated. When the other reagents are used, the evaluation must be done using another method (e.g. grid-based quantitative analysis). Sigma phase proportions found by optical microscopy are higher than those measured using EBSD. In order to identify microstructural variations across the forged parts, specimens were taken from three locations (centre, ¼ , edge). The sigma phase amounts found in all three testing locations of the sample of the cerium-doped duplex steel were higher than the corresponding amounts in the cerium-free sample. In both materials, the amounts of sigma phase are higher in the centre of the sample than near the edge. This difference is more significant in the cerium-free material.

Originality/value: The article is devoted to phase content evaluation in duplex steels by different methods. EBSD and image analysis of micrographs were compared. Micrographs were acquired by light microscopy after microstructure revelation by various etchants. The content of ferrite, austenite and intermetallic phases was evaluated.

Keywords: Duplex steels; Etching techniques

Reference to this paper should be given in the following way:

P. Martínek, P. Podaný, Etching techniques for duplex steels, Journal of Achievements in Materials and Manufacturing Engineering 68/1 (2015) 11-16.

MATERIALS

1. Introduction

The history of duplex steels, i.e. two-phase austenitic-ferritic stainless steels, is almost as long as that of stainless steels but the interest of the industry in this group of steels has been increasing recently. This mainly holds for applications where austenitic steels do not provide a guarantee of fault-free and safe operation, particularly in environments where stress-corrosion cracking may occur [1]. Duplex stainless steels are frequently used in industry for their excellent combination of mechanical properties and corrosion resistance. Their resistance to uniform corrosion is similar to austenitic steels but their strength is much higher [2]. These characteristics depend on the two-phase microstructure that comprises austenite and delta ferrite [1]. Ferrite enhances strength and imparts resistance to stress-corrosion cracking. However, ferrite is also prone to microstructural changes whereas austenite remains the stable phase. As a result, these steels develop undesirable intermetallic phases in the critical temperature range of 650-900°C during forging or rolling earlier than austenitic steels [3, 4]. This applies primarily to the sigma phase (σ) which is hard, brittle, non-magnetic and stable. Precipitation of sigma phase in steel increases the brittleness, hardness, ultimate and yield strengths whereas the elongation and reduction of area in ambient-temperature tensile test decrease.

In order to make products that provide trouble-free operation, one needs to have detailed knowledge of the microstructure of duplex steels. The proportions of major phases must be known, as well as their amounts, sizes, distributions and also the types of intermetallic phases, if present. To facilitate mapping of these characteristics, the present experiment was proposed. Its aim was to identify the most appropriate etching technique for these steels to meet the aforementioned need.

2. Experimental

The samples used for examination were forged bars whose microstructures were in two conditions. One of them was an open-die forged and solution-annealed condition. The forging operations were performed between 1200°C and 900°C. The soaking time at the forging temperature was 10 hours. The solution annealing was carried out at 1050°C for 4 hours with subsequent quenching in water. The other condition of the samples was achieved by the same procedure with additional annealing at 750°C for 48 hours and subsequent cooling in air. The goal was to induce extensive precipitation of intermetallic phases. In the forged and solution-annealed specimens, the fractions of austenite and ferrite were evaluated. In long-time-annealed specimens, the evaluation focused primarily on intermetallic phases. With the aim of identifying microstructural variations across the forged parts, specimens were taken from three locations (centre, ¼, edge) - as shown in Fig. 1.

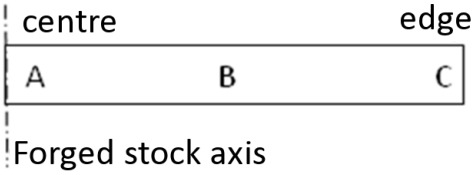

Fig. 1. Specimen codes

The experimental materials were X2CrNiMoN 22-5-3 steel and its cerium-doped variant (the specimen code included the letters Ce).

2.1. Optical microscopy

The microstructures of the duplex steel specimens were revealed using several reagents which fall into two groups. The first one comprises chemical reagents: Beraha II+ $K_2S_2O_5$, Beraha II and Murakami's reagent. The second includes electrolytic etchants: NaOH, NH_4OH, 60% HNO_3 and oxalic acid. Once the microstructure was revealed, the fractions of individual microstructure constituents were evaluated. The number of fields of view used for the evaluation was 20 in both groups of specimens and for all etchants.

An effort was made to employ NIS Elements 3.2 image analysis software for the evaluation in all cases.

In solution-annealed specimens, the phase composition was evaluated by image analysis upon etching with the following reagents: Beraha II+$K_2S_2O_5$, NaOH and Murakami's reagent. The other etchants used (oxalic acid, 60% HNO_3 and Beraha II) proved unsuitable for quantitative image analysis evaluation, as they did not provide sufficient contrast between phases.

In the long-time-annealed specimens, quantitative image analysis could only be used for evaluating the phase composition upon etching with NaOH solution or NH_4OH or Murakami's reagent. When the other etchants (Table 1) were used, grid-based quantitative analysis had to be employed. In the grid-based analysis, 20 fields of view were used as well.

Table 1.
Sigma phase fractions in long-time-annealed specimens [%]

Specimen	Etching reagent		
	Beraha II + $K_2S_2O_5$	NaOH	Beraha II
	σ+chi phase fraction	σ+chi phase fraction	σ+chi phase fraction
A	18.94 ± 1.56	20.25 ± 1.39	17.50 ± 1.16
B	20.58 ± 2.87	18.99 ± 1.90	not evaluated
C	13.84 ± 1.43	15.75 ± 1.28	14.67 ± 1.28
Ce A	22.05 ± 2.04	23.50 ± 1.53	21.16 ± 1.43
Ce B	19.57 ± 1.77	20.18 ± 1.54	not evaluated
Ce C	21.26 ± 1.67	19.69 ± 1.20	21.06 ± 1.39

Specimen	Etching reagent	
	Murakami	NH_4OH
	σ+chi phase fraction	σ+chi phase fraction
A	not evaluated	20.03 ± 1.04
B	18.08 ± 1.42	0.94 ± 0.94
C	12.80 ± 1.40	1.00 ± 1.00
Ce A	not evaluated	21.86 ± 1.46
Ce B	21.24 ± 1.66	1.36 ± 1.36
Ce C	19.19 ± 1.36	1.24 ± 1.24

2.2. EBSD analysis

Crystallographic data on the specimens were gathered using EBSD (Electron Backscatter Diffraction). This method relies on analysing Kikuchi lines obtained by directing an electron beam on a specimen tilted under a large angle in the chamber of a scanning electron microscope (SEM). Using the EBSD method, the fractions of phases were determined. The values were then compared to the data obtained using optical microscopy. The scope of measurement in each method was different. Under the optical microscope, the phase fractions were determined from 20 fields of view at a magnification of 500. For the EBSD analysis, five fields of view were used, each with the size of 400×200 µm. By area, one field of view in EBSD analysis approximately corresponds to 3.5 fields of view under the optical microscope at the 500× magnification. The aggregate areas evaluated by optical microscopy and EBSD are thus roughly comparable. An example EBSD map used for evaluating the sigma phase fraction is shown in Fig 2. The phase composition found by EBSD is listed in Table 2.

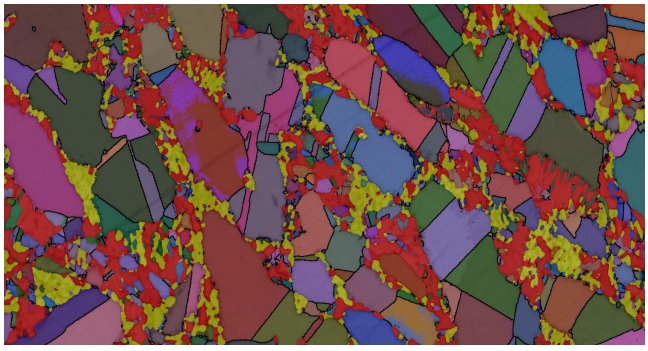

Fig. 2. Specimen C - upon long-time annealing. EBSD analysis; ferrite appears red. σ phase appears yellow. Austenite - colours depending on orientation

Table 2.
Phase fractions found by EBSD in long-time-annealed specimens [%]

Specimen	Ferrite	Austenite	σ+chi
A	12.5	72.8	14.7
B	9.2	75.6	15.2
C	17.7	71.2	11.1
Ce A	7.5	68.3	24.2
Ce B	21.0	68.1	19.9
Ce C	5.8	75.1	19.1

3. Discussion

3.1. Solution-annealed specimens

Duplex steels can be etched both chemically and electrolytically using several different etchants. In the solution-annealed specimens, no intermetallic phases were found using either optical or scanning electron microscopy. Therefore, only the ferrite and austenite fractions were evaluated for the solution-annealed specimens.

The differences between phase fractions found after etching with different reagents are small and close to the measurement error. The ferrite amount is between 43 and 46%. Table 3 shows that the amount of ferrite found upon etching with NaOH was higher than with the other two reagents. It can be explained by the fact that etching with NaOH produces a relatively thick oxide layer on ferrite grains. This layer thus overhangs other phases and distorts the data.

The Beraha II+$K_2S_2O_5$ reagent is a colour etchant which produces a thin oxide layer on the specimen surface. This

layer is usually non-uniform. Additional etching is impossible with this reagent. Etching with Murakami's solution is carried out at an elevated temperature and the etching time is longer than with other reagents (Fig 3). Etching with NaOH does not involve such disadvantages - Fig. 4. It is an electrolytic process which was found to be the most feasible one. On the other hand, it may lead to a slight distortion of results.

The average amounts of ferrite across all reagents and measurement areas in cerium-free and cerium-doped specimens were 42.6% and 45.6%, respectively. The difference between the two materials is approximately three percentage points. This difference is probably the consequence of the difference in their chemical compositions. No differences were found between locations from which specimens were taken.

Table 3.
Ferrite amounts in solution-annealed samples [%]

Specimen	Etching reagent		
	Beraha II + $K_2S_2O_5$	NaOH	Murakami
	Ferrite fraction	Ferrite fraction	Ferrite fraction
A	41.45 ± 0.73	43.65 ± 0.68	42.70 ± 1.07
B	41.32 ± 0.75	43.80 ± 0.80	41.09 ± 0.70
C	43.88 ± 0.46	43.87 ± 0.69	41.94 ± 0.66
Ce A	47.02 ± 0.80	46.32 ± 1.00	45.66 ± 0.98
Ce B	43.96 ± 0.67	45.44 ± 0.69	45.97 ± 0.66
Ce C	44.63 ± 0.68	45.60 ± 0.63	46.12 ± 0.73

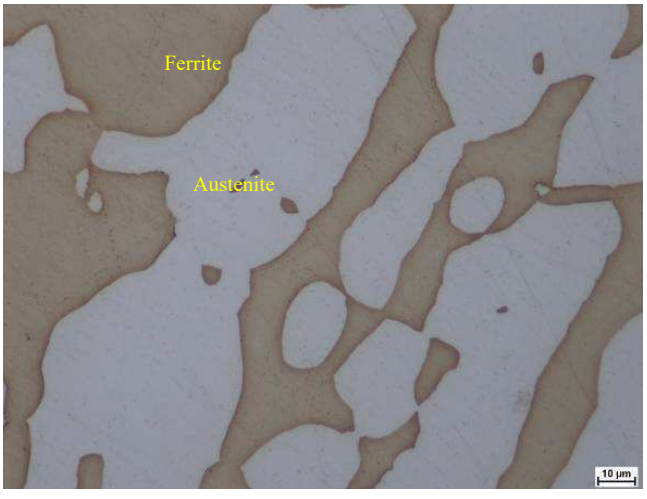

Fig. 3. Specimen CeB - upon solution-annealing. Etched with Murakami's reagent

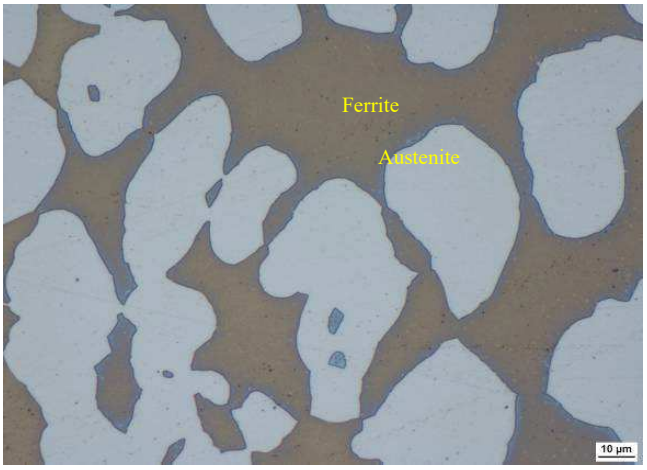

Fig. 4. Specimen A – upon solution-annealing. Etched with NaOH solution

3.2. Long-time-annealed specimens

Long-time annealing led to extensive precipitation of intermetallic phases. Carbides were not evaluated using optical microscopy and image analysis. Although they were readily visible upon etching with some reagents, they were too small for quantitative evaluation. This is why the amounts of sigma phase and chi phase were the main variables evaluated for various reagents. Both phases are very similar in terms of their properties. They are impossible to distinguish from each other using optical microscopy. Another reason why both phases were evaluated as a single one and denoted in the tables below as "sigma phase" is that their effects on the properties of duplex steels are similar.

The etch with Beraha II+$K_2S_2O_5$ or Beraha II revealed both major phases and sigma phase relatively well. However, carbides and austenite grain boundaries were not visible.

When NaOH, NH_4OH and Murakami's reagent were used, particles of sigma phase became prominent and well-suited for image analysis; and carbides on grain boundaries were visible (Figs. 5-8). However, as Table 1 suggests, the highest fraction of sigma phase was found upon the NaOH etch (Fig. 6). Etching with this solution produces a relatively thick oxide layer on the surface. This oxide layer causes the measured values for a particular phase to be higher than the actual values. The advantage of this reagent lies in that the sigma phase proportion can be effectively measured by mean of image analysis.

Upon etching with nitric acid or oxalic acid, sigma phase could only be evaluated using the grid-based analysis

but not by image analysis. Austenite grains and carbides on their boundaries were well visible.

The sigma phase amounts found in all three testing locations of the sample of the cerium-doped duplex steel were higher than the corresponding amounts in the cerium-free sample. This is probably due to the higher ferrite amount in this material, as sigma phase nucleates more readily in ferrite than in austenite.

In both materials, the amounts of sigma phase were higher in the centre of the sample than near the edge. This difference was more significant in the cerium-free material.

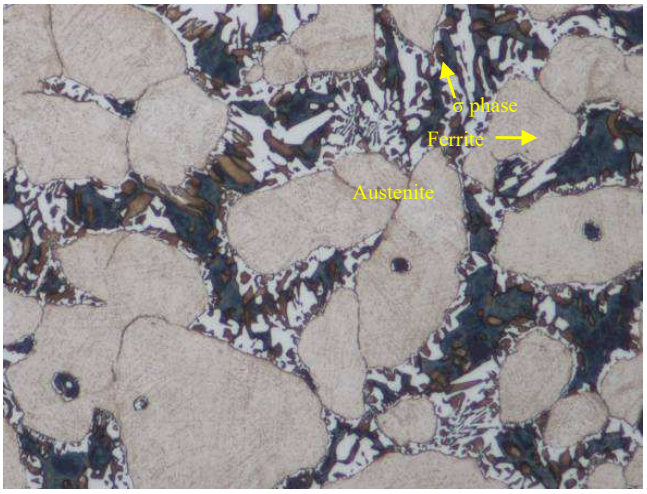

Fig. 5. Specimen A - upon long-time annealing. Etched with Beraha II+$K_2S_2O_5$

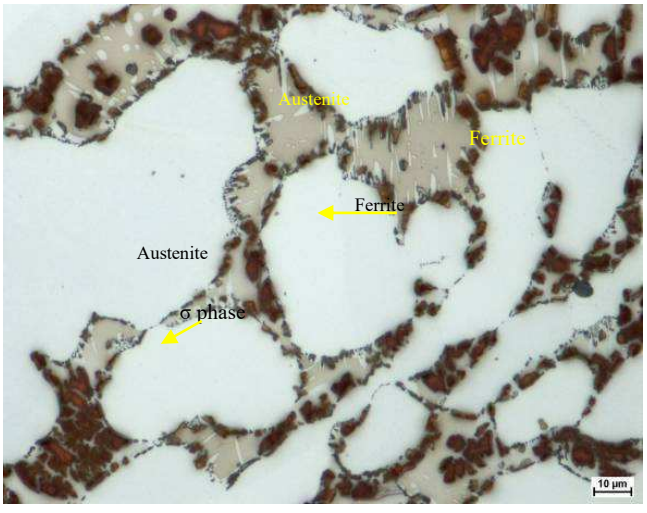

Fig. 6. Specimen A - upon long-time annealing. Electrolytic NaOH etch

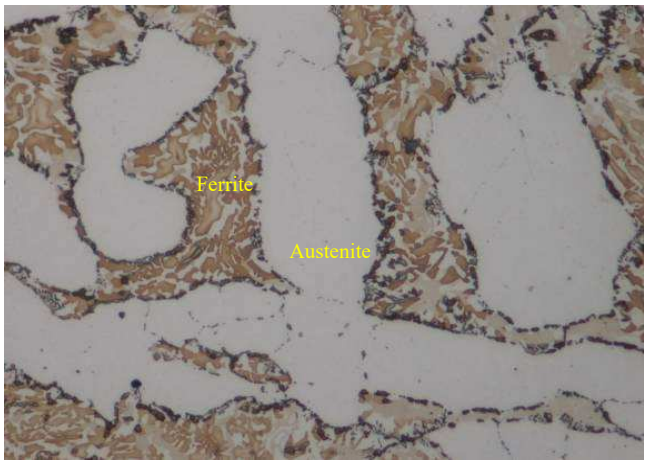

Fig. 6. Specimen C - upon long-time annealing. Etched with Murakami's reagent

Fig. 8. Specimen CeC - upon long-time annealing. Etched with Beraha II

3.3. Comparison of results obtained using optical microscopy and EBSD

The comparison of data shown in Tables 2 and 3 revealed that EBSD analysis yielded lower sigma phase values than image analysis. The possible causes are given below.

When the amount of a certain phase is evaluated using optical microscopy and image analysis, the value tends to be overestimated. This is due to both human factor and etching products. Those form on the surface of the phase

by chemical or electrochemical reactions. They may have relatively large thickness and may extend beyond the phase in question, thus distorting the measurement.

On the other hand, the EBSD outcomes depend on the quality of diffraction patterns of individual phases. As the sigma phase particles are small and the diffraction is less clear on the interphase interfaces, the sigma phase is not identified on the entire area. As a result, its area fraction values are underestimated.

The eutectoid decomposition of ferrite produces sigma phase and small austenite grains which are difficult to discern under the optical microscope. Consequently, they tend to be included in the sigma phase area. EBSD analysis, however, allows even these small grains to be identified.

4. Conclusions

The purpose of this study was to find the optimum etching technique for duplex steels which would enable a metallographer to determine the amounts of delta ferrite and austenite and the fractions, distributions and types of intermetallic phases using image analysis. The values obtained by means of optical microscopy were compared to the EBSD data. The results can be summarised as follows.

In X2CrNiMoN 22-5-3 duplex steel, the microstructure can be revealed using various reagents and both chemical and electrochemical etching.

The differences between the reagents when used for evaluating the amounts of major phases (austenite +ferrite) were not substantial.

The fraction of sigma phase in long-time-annealed samples can be evaluated using image analysis only if etched with NaOH solution or NH_4OH. These etchants also effectively reveal carbides on grain boundaries. However, the values obtained with NaOH are overestimated. When the other reagents are used, the evaluation must be done using another method (e.g. grid-based quantitative analysis).

Sigma phase proportions found by optical microscopy are higher than those measured using EBSD.

In order to identify microstructural variations across the forged parts, specimens were taken from three locations (centre, ¼, edge). The sigma phase amounts found in all three testing locations of the sample of the cerium-doped duplex steel were higher than the corresponding amounts in the cerium-free sample.

In both materials, the amounts of sigma phase are higher in the centre of the sample than near the edge. This difference is more significant in the cerium-free material.

Acknowledgements

This paper was prepared under the project entitled Development of West-Bohemian Centre of Materials and Metallurgy No.: LO1412, which is funded by the Ministry of Education of the Czech Republic.

References

[1] M. Liljas, 80 years with duplex steels, a history review and prospects for the future, http://www.euroinox.org /pdf/map/paper/Duplex_Steels_EN.pdf
[2] Stainless Steel Conference Science and Market, ISBN 91-974131-9-4, Helsinki, Finland, 2008.
[3] Information on http://www.mmspektrum.com.
[4] T. Chen, K. Weng, J. Yang, The effect of high-temperature exposure on the microstructural stability and toughness property in a 2205 duplex stainless steel Materials Science and Engineering, 338/1-2 (2002) 259-270.
[5] G. Kaishu, Effect of aging at 700°C on precipitation and toughness of AISI 321 and AISI 347 austenitic stainless steel welds, Nuclear Engineering and Design 235 (2005) 2485-2494.
[6] J.C. Dutra, F. Siciliano, A.F. Padilha, Interaction between second-phase particle dissolution and abnormal grain growth in an austenitic stainless steel, Materials Research 5/3 (2002) 379-384.